# COMSOL Simulation of a Dual-axis MEMS Accelerometer with T-shape Beams

Ce Zheng[1], Xingguo Xiong[2], Junling Hu[3],
[1] Department of Electrical Engineering, University of Bridgeport, Bridgeport, CT, USA
[2] Department of Electrical and Computer Engineering, University of Bridgeport, Bridgeport, CT, USA
[3] Department of Mechanical Engineering, University of Bridgeport, Bridgeport, CT, USA

**Abstract:** Inertial navigation in 3D space requires acceleration measurement along all three degree-of-freedoms. For improved efficiency, accelerometers which can sense acceleration along multiple axes are desired. In this paper, a dual-axis MEMS (Microelectromechanical Systems) accelerometer with T-shape beam structure is proposed. When there is acceleration input along X and Y directions, the T-shape beams bend accordingly due to inertial force. The bending displacement along X and Y directions can be measured by differential capacitance sensing, hence the input accelerations can be derived. COMSOL Multiphysics is used to simulate the displacement sensitivity of the accelerometer along X and Y directions. Solid Mechanics (solid) physics and Electromechanics (emi) physics are used in device modeling. Stress intensity simulation of the device under input acceleration of 50g is also performed. The designed dual-axis MEMS accelerometer can be further integrated with a Z-axis accelerometer for complete 3D inertial navigation.

**Keywords:** COMSOL multiphysics, Microelectromechancial Systems (MEMS), Dual-axis accelerometer, Differential capacitive sensing, Inertial navigation system.

## 1. Introduction

Due to their small size, light weight, low cost and low energy consumption, MEMS (Microelectromechanical Systems) accelerometers have been widely used in smart phones, automobile, toys, aerospace and many other applications [1]. Most MEMS accelerometers are designed to sense acceleration input along single direction. For complete inertial navigation in 3D space, measurement of acceleration inputs along all three directions (X, Y and Z) is required. Hybrid integration of three single-axis accelerometers aligned along each direction is a straight-forward solution. However, it requires precise alignment and calibration of three separate accelerometers, which can be very challenging. A more efficient solution is to design accelerometer which can measure acceleration along multiple axes. Various dual-axis MEMS accelerometers have been reported [2]-[6]. In [2], a MEMS dual-axis capacitive accelerometer with pendulum-proof-mass, a gimbal-spring and vertical-combs sensing electrodes is proposed. In [3], a dual-axis accelerometer with a single inertial mass symmetrically suspended by four pairs of folded elastic beams is reported. The four pairs of folded beams allow the movable mass to move along both X and Y directions due to inertial force. In [4], a high-sensitivity dual-axis linear accelerometer is fabricated with CMOS-MEMS technology. In [5], a dual-axis MEMS inertial sensor that utilizes multi-layered electroplated gold for an arrayed CMOS-compatible MEMS accelerometer is reported. It allows both the signal sensing circuitry and the sensing units to be fabricated on the same chip. In [6], a dual-axis MEMS thermal accelerometer made with front-side bulk micromachining and CMOS technology is introduced. The accelerometer utilizes thermal convection phenomenon to sense the input acceleration.

In this research, a MEMS dual-axis capacitive accelerometer with T-shape beams is proposed. It utilizes only two sets of T-shape beams to sense acceleration inputs along both X and Y direction in device plane. Each T-shape beam contains two folded beams and one straight beam. The T-shape structure allows the beams to bend along both X and Y directions due to input acceleration. The bending displacement of the beams is sensed by the differential capacitance change of the comb finger groups connected to the central movable mass. COMSOL Multiphysics is used to simulate the sensitivities of the accelerometer along X and Y directions. The contour plot of the stress intensity distribution for 50g acceleration input is also obtained. The proposed MEMS dual-axis accelerometer can be combined with a Z-axis accelerometer for complete 3D inertial navigation system.

## 2. Design and Analysis

### 2.1 Structural Design of Dual-axis MEMS Accelerometer with T-shape Beams

The structure diagram of the dual-axis MEMS comb accelerometer is shown in Figure 1. It is to be fabricated with polysilicon surface-micromachining. It has two T-shape beams connected to movable mass. The whole device is symmetric vertically and horizontally. Each T-shape beam consists of one straight beam and 2 folded beams connected between the anchor and the central mass. There are eight groups of movable fingers extruding from the four sides of the movable mass. To simplify the analysis, the two straight beams and four vertical finger groups are used to sense acceleration along X direction, so they are called X-beams and X-capacitance groups. The four folded beams and four horizontal finger groups are used to sense acceleration along Y direction, so they are called Y-beams and Y-capacitance groups. As shown in the figure, among the four groups of X-movable fingers, two groups of them have fixed fingers in their left sides and other two groups have fixed fingers in their right sides. Together they constitute X-differential capacitance. Similarly, among the four groups of Y-movable fingers, two groups of them have fixed fingers in their upper sides and other two groups have fixed fingers in their down sides. Together they constitute Y-differential capacitance. By designing the fixed fingers to be only in one side of the movable fingers, the interconnects for left and right (or top and bottom) fixed fingers will not cross each other. This makes the fabrication process easier.

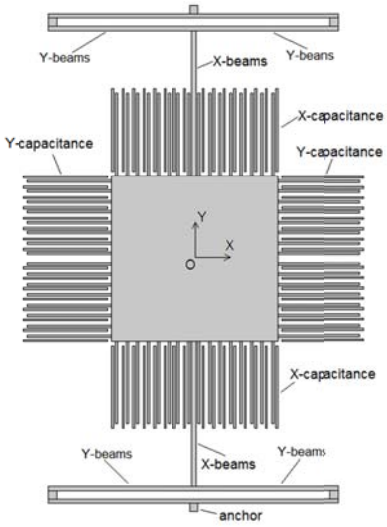


Figure 1. Structure diagram of dual-axis MEMS accelerometer

The working principle of the dual-axis MEMS accelerometer is explained as below. If there is acceleration input $a_x$ along X direction, the straight X-beams bend due to inertial force, hence the X-differential capacitance changes. By measuring this X-differential capacitance changes, the input acceleration $a_x$ can be calculated. On the other hand, if there is acceleration $a_y$ along Y direction, the folded Y-beams bend and Y-differential capacitance changes. By measuring the Y-differential capacitance change, we know the input acceleration $a_y$. Table 1 shows all the design parameters of the device. The thickness of polysilicon structure is set as t=4μm.

**Table 1. Design Parameters of MEMS Accelerometer**

| Components | Amount | Length (μm) | Width (μm) | Numbers in figure |
|---|---|---|---|---|
| Central mass | 1 | 800 | 800 | 9 |
| Movable fingers | 64 (8×8) | 400 | 10 | 7 |
| Fixed fingers | 64 | 400 | 10 | 8 |
| Folded beam segments | 8 | 700 | 20 | 2,3,4,5 11,12,13,14 |
| Straight beams | 2 | 700 | 20 | 6,10 |
| Anchors | 2 | 40 | 40 | 1,15 |

### 2.2 Theoretical Analysis

The dual-axis MEMS accelerometer with T-shape beams utilizes differential capacitance to sense the displacement of the movable mass/fingers due to inertial force. In this device, the folded beams can only bend along Y direction, and the straight beams can only bend along X direction. This ensures the cross-axis coupling effect of the accelerometer is minimized. When there is no acceleration input, the left capacitance gap is equal to the right capacitance gap ($d_1=d_2=d_0$) for X-capacitances, and the top capacitance gap is equal to the bottom capacitance gap ($d_3=d_4=d_0$) for Y-capacitances. As a result, the left X-capacitance equals to right X-capacitance ($C_1=C_2=C_{x0}$), and top Y-capacitance equals to bottom Y-capacitance ($C_3=C_4=C_{y0}$).

When there is acceleration along X-axis direction, due to inertial force, the movable fingers move toward left by displacement x, then: $d_1'=d_0-x$, $d_2'=d_0+x$, the X-capacitance change is

$$\Delta C_x = C_1' - C_2' \approx 2\Delta C_1 = 2\frac{N_x \varepsilon S}{d_0} \cdot \left(\frac{x}{d_0}\right) \qquad (1)$$

where $N_x$ is the number of X-differential capacitance groups, ε is permittivity of air, S is the overlap area between a movable finger and its left (or right) fixed finger ($S=t\times L_{ov}$, in it $t$ is the device thickness and $L_{ov}$ is the overlap length between movable and fixed fingers), $d_0$ is the static capacitance gap of X-capacitance.

When there is acceleration along Y-axis direction, assume movable fingers move toward bottom by displacement y due to inertial force. As a result, $d_3'=d_0+y$, $d_4'=d_0-y$, the Y-differential capacitance change is

$$\Delta C_y = C_3' - C_4' \approx 2\Delta C_3 = 2\frac{N_y \varepsilon S}{d_0} \cdot \left(\frac{y}{d_0}\right) \quad (2)$$

where $N_y$ is the number of Y-differential capacitance groups, S is the overlap area between a movable finger and its top (or bottom) fixed finger, $d_0$ is the static capacitance gap of Y-capacitance.

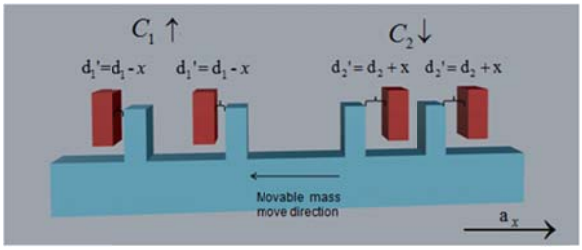


Figure 2. Differential capacitance sensing for acceleration along X-axis

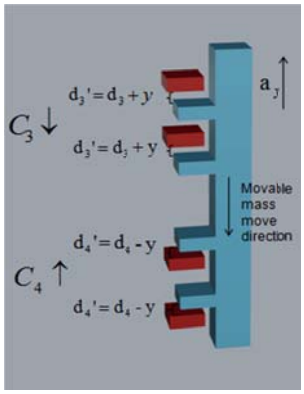


Figure 3. Differential capacitance sensing for acceleration along Y-axis

From above analysis, we can see that under small deflection approximation (i.e. $x \ll d_0$ or $y \ll d_0$), the differential capacitance output ΔC has approximately linear relationship with displacement of movable fingers. Furthermore, the bending displacement of the beams is proportional to the inertia force $F_{inertial}$, which is also proportional to input acceleration:

$$F_{inertial} = -M_s \cdot a \quad (3)$$

$$x = F_{inertial}/K_{xtot} \quad (4)$$

$$y = F_{inertial}/K_{ytot} \quad (5)$$

where $M_s$ is the mass of the sensing mass, and $a$ is the input acceleration, $K_{xtot}$ and $K_{ytot}$ are the effective spring constants of the beams along X and Y directions. Thus the differential capacitance change ΔC is linearly proportional to the input acceleration. By measuring the differential capacitance change, we can know the input acceleration.

The effective spring constants of the device along X and Y directions can be calculated as

$$K_{xtot} = 2E \cdot w_{bx}^{\ 3} \cdot t_{bx} \Big/ L_{bx}^{\ 3} \quad (6)$$

$$K_{ytot} = 2E \cdot w_{by}^{\ 3} \cdot t_{by} \Big/ L_{by}^{\ 3} \quad (7)$$

where E is the Young's modulus of the device material (for polysilicon, E=169GPa [7]), $w_{bx}$, $t_{bx}$ and $L_{bx}$ are the width, thickness and length of straight X-beams respectively, $w_{by}$, $t_{by}$ and $L_{by}$ are the width, thickness and length of folded Y-beams respectively. Assume uniform device thickness t, we have $t_{bx}=t_{by}=t$.

Resonant frequencies for vibration along X and Y directions are:

$$f_x = \frac{1}{2\pi}\sqrt{\frac{2E \cdot w_{bx}^{\ 3} \cdot t_{bx}}{L_{bx}^{\ 3} \cdot \rho\left(w_m \cdot L_m \cdot t_m + 64 \cdot w_f \cdot L_f \cdot t_f\right)}} \quad (8)$$

$$f_y = \frac{1}{2\pi}\sqrt{\frac{2E \cdot w_{by}^{\ 3} \cdot t_{by}}{L_{by}^{\ 3} \cdot \rho\left(w_m \cdot L_m \cdot t_m + 64 \cdot w_f \cdot L_f \cdot t_f\right)}} \quad (9)$$

where $w_m$, $L_m$ and $t_m$ are the width, length and thickness of central mass, $w_f$, $L_f$ and $t_f$ are the width, length and thickness of movable fingers. Actually $t_m=t_f=t$ (device thickness).

The displacement sensitivity is defined as the displacement of the movable fingers per 1g acceleration input (g is gravity acceleration, 1g=9.8m/s$^2$) along sensitive direction. The displacement sensitivities of the accelerometer along X and Y directions are:

$$S_{dx} = \frac{\rho\left(w_m \cdot L_m \cdot t_m + 64 \cdot w_f \cdot L_f \cdot t_f\right) \cdot g \cdot L_{bx}^{\ 3}}{2E \cdot w_{bx}^{\ 3} \cdot t_{bx}} \quad (10)$$

$$S_{dy} = \frac{\rho\left(w_m \cdot L_m \cdot t_m + 64 \cdot w_f \cdot L_f \cdot t_f\right) \cdot g \cdot L_{by}^{\ 3}}{2E \cdot w_{by}^{\ 3} \cdot t_{by}} \quad (11)$$

Based on the above analysis, it can be seen that adjusting the beam width is an effective way to set the displacement sensitivity without affecting the overall device area. Based on Equation (10), with other design parameters fixed, the relationship between displacement sensitivity $S_{dx}$ and the width of straight X-beams ($w_{bx}$) can be plotted in Figure 4. The sensitivity $S_{dx}$ is reversely proportional to $t_{bx}^3$. As $t_{bx}$ is reduced, $S_{dx}$ goes up very quickly.

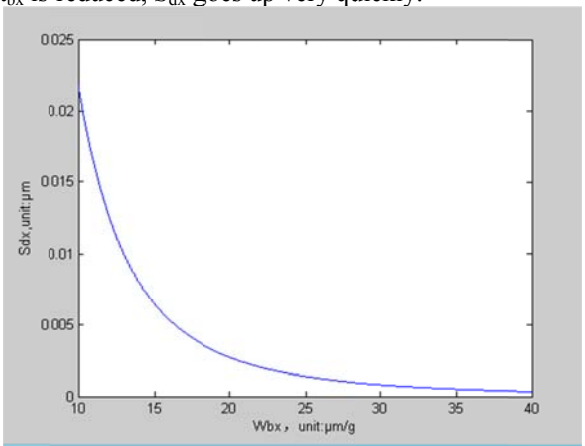


Figure 4. Sensitivity ($S_{dx}$, unit: $10^{-4}$ μm/g ) vs width of X-beams ($w_{bx}$, unit: μm)

Similarly, the relationship between displacement sensitivity $S_{dy}$ and the width of folded Y-beams ($w_{by}$) is plotted in Figure 5.

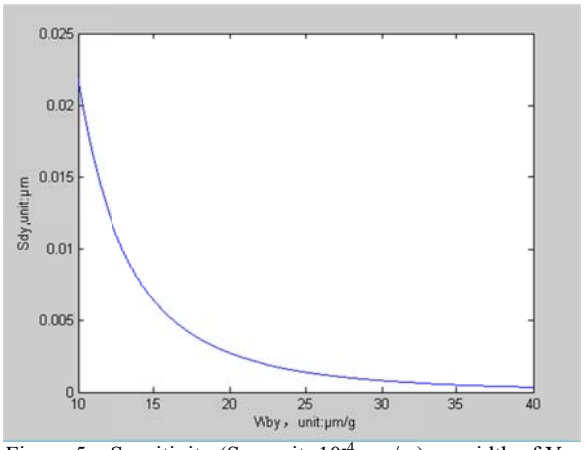


Figure 5. Sensitivity ($S_{dy}$, unit: $10^{-4}$ μm/g ) vs width of Y-beams ($w_{by}$ , unit:μm)

## 3. Use of COMSOL Multiphysics

COMSOL Multiphysics is used to simulate the displacement sensitivity of the dual-axis accelerometer along X and Y directions. The 3D model of the dual-axis accelerometer device is shown in Figure 6. Solid Mechanics (solid) physics and Electromechanics (emi) physics are used for device model. Stationary study is performed for device simulation. The input acceleration is defined by introducing an inertial force as a body load $F_v$, which is the force per unit volume due to input acceleration:

$$F_v = F_{inertial} = -\rho \cdot a \qquad (12)$$

where ρ is the density of device material, a is the input acceleration.

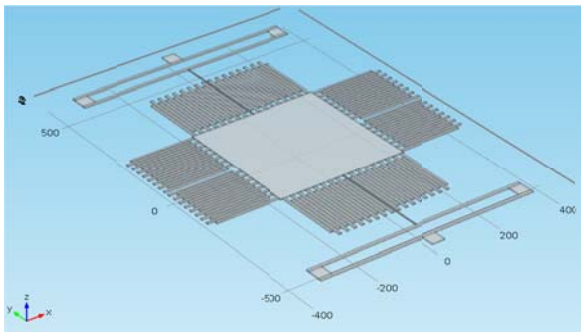


Figure 6. COMSOL model of dual-axis MEMS accelerometer with T-shape beams

The complete device model of the dual-axis MEMS accelerometer is designed in COMSOL. Polysilicon is used as the material of the device. The device structure consists of two parts: movable part and stationary part. Stationary part includes all the fixed comb fingers as well as the two anchors. The movable part includes the T-shape beams, movable mass and all the movable fingers. The meshing size is set to be coarse. With all the fixed constraints and input accelerations defined, stationary study is performed to find the displacement sensitivity and stress intensity distribution of the accelerometer.

### 3.1. Sensitivity Simulation

We apply unit gravity acceleration (1g=9.8m/s$^2$) to simulate the sensitivity along X and Y directions respectively. Figure 7 shows the COMSOL sensitivity simulation result for 1g acceleration along X direction. From the contour plot we can see that the displacement sensitivity of the acceleration along X-direction is $S_{dx}$=0.0051578μm/g.

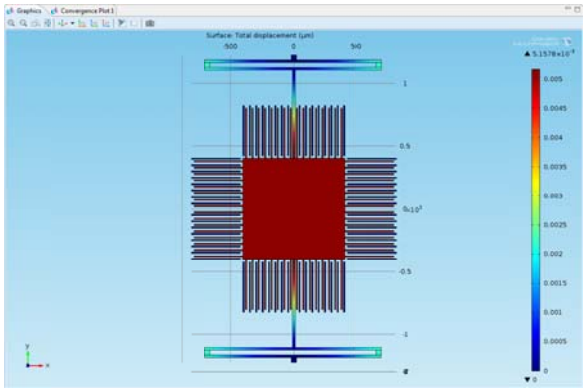

Figure 7. COMSOL simulation result of displacement sensitivity along X-axis

The detailed bending shape of the straight X-beam is shown in Figure 8. We can see that the bending displacement increases along the straight X-beam, and the maximum displacement is achieved at the end of the beam, as well as the movable mass and all movable fingers.

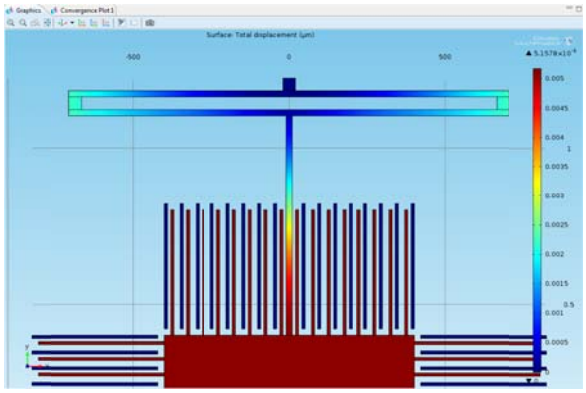

Figure 8. Displacement sensitivity along X-axis (detail)

The COMSOL simulation of displacement sensitivity along Y direction is shown in Figure 9. We can see that the folded beams bend along Y direction due to inertial force. According to the result, the displacement sensitivity along Y direction is $S_{dy}$=0.0026694μm/g.

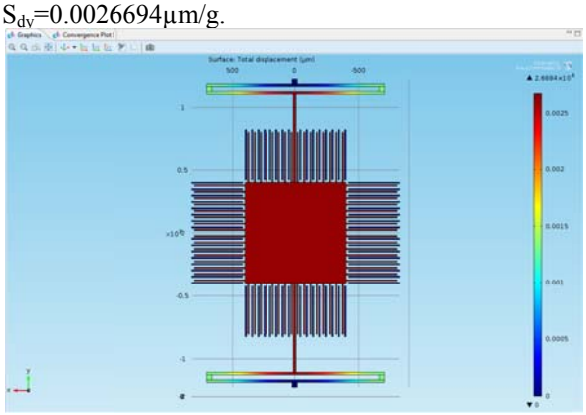

Figure 9. Displacement sensitivity along Y-axis

The detailed bending shape of the folded Y-beam is shown in Figure 10. We can see that the maximum bending displacement occurs at the end of the folded beams.

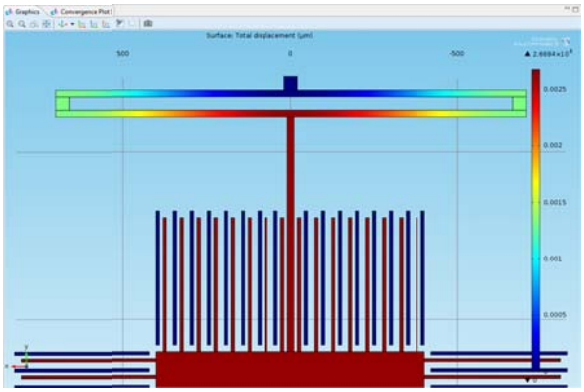

Figure 10. Displacement sensitivity in Y-axis (detail)

Based on the above simulation results, the displacement sensitivities of the dual-axis MEMS accelerometer along X and Y axes are found to be $S_{dx}$=0.0051578μm/g and $S_{dy}$=0.0026694μm/g respectively.

### 3.2. Stress Simulation

Stress simulation is performed to find out the stress induced inside the material when the beams bend due to maximum full-scale acceleration input. If the maximum stress in device is more than the material strength of polysilicon, the material will crack and the device is out of function. We apply acceleration input of 50g along X and Y directions to simulate the stress distribution inside the accelerometer in COMSOL. The results are shown in Figures 11-14.

When acceleration of 50g is applied along X direction, the stress intensity plot of the device is shown in Figure 11.

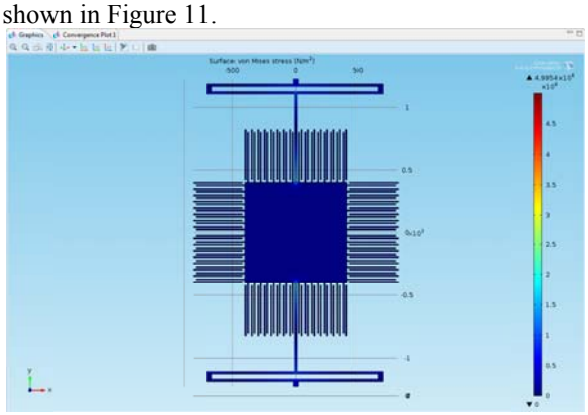

Figure 11. Stress intensity plot for $a_x$=50g along X-axis

We can see that the stress mainly occurs inside the straight X-beams, and all the other parts of the device experiences almost zero stress. The stress is induced by the deformation of the X-beams. To see more detailed stress distribution along the straight X-beams, the portion is zoomed in and shown in Figure 12.

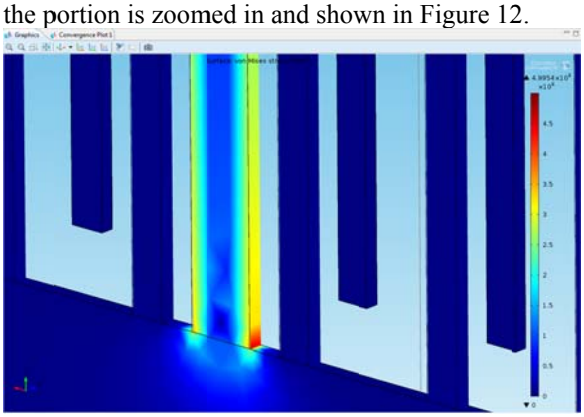

Figure 12. COMSOL stress intensity for acceleration $a_x$=50g (zoomed along end of X-beam)

When acceleration of 50g is applied along Y direction, the stress intensity contour plot of the device is shown in Figure 13. The stress mainly occurs in the folded Y-beams.

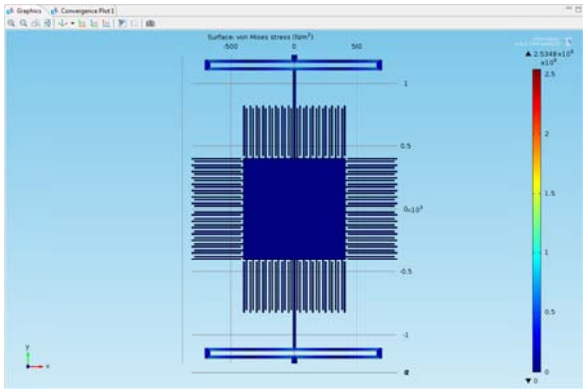

Figure 13. Stress intensity plot for $a_y$=50g along Y-axis

We can see that the stress mainly occurs inside the straight Y-shape beams. To see more detailed stress distribution along the straight Y-beams, the portion is zoomed in and shown in Figure 14.

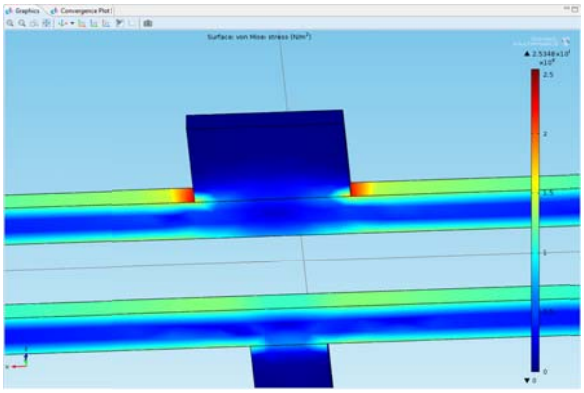

Figure 14. Stress intensity plot for $a_y$=50g (zoomed along the root of Y-beams)

Based on COMSOL simulation result, we found the maximum stress intensity is $4.5594\times10^6$ Pa and $2.5348\times10^6$Pa for 50g acceleration along X and Y directions respectively. According to [8], the fracture strength of polysilicon is (2.9±0.5) GPa in tensile testing and (3.4±0.5) GPa in bending tests. In long-term investigations, the fracture strength of poly-silicon was observed to have a slightly decrease to 2.2 GPa over $10^6$ cycles [8]. For 50g acceleration inputs along both X and Y directions, the maximum stress intensity is well below the material fracture strength of poly-silicon. Thus the device is safe during full-range operation. COMSOL simulation also shows that the maximum stress occurs at the root of straight X-beams connecting to movable mass, as well as the end of the folded beams connecting to the anchors. For long-term reliability, these two parts should be enhanced in device design.

## 4. Conclusions

In this paper, a dual-axis MEMS accelerometer with T-shape beams is introduced. T-shape beam structure allows the accelerations along both X-axis and Y-axis to be measured by differential capacitance sensing. COMSOL Multiphysics is used to simulate the displacement sensitivities of the accelerometer along X and Y directions. Stress intensity plots were also obtained for 50g acceleration inputs along X and Y directions. Solid Mechanics (solid) physics and Electromechanics (emi) physics are used in device modeling. Compared to the hybrid integration of multiple sensors, dual-axis accelerometer can reduce the fabrication cost and improve efficiency. It can be further integrated with a Z-axis accelerometer for complete 3D inertial navigation.

## References


[1] D.K. Shaeffer, "MEMS inertial sensors: A tutorial overview", in Communications Magazine, IEEE, Vol. 51, Issue 4, 2013, pp. 100-109.

[2] C.-K. Chan, C.-P. Hsu, M. Wu, H. Hocheng, R. Chen, W. Fang, "A novel differential capacitive-sensing dual-axis accelerometer design using pendulum-proof mass, gimbal-springs, and harm vertical-combs", International Solid-State Sensors, Actuators and Microsystems Conference, 2009 (TRANSDUCERS 2009), pp. 1944-1947.

[3] W. Chen, J. Ding, X. Liu, C. Wang, "Design and system-level simulation of a capacitive dual axis accelerometer", 2nd IEEE International Conference on Nano/Micro Engineered and Molecular Systems (NEMS'07), 2007, pp. 614-617.

[4] A. Baschirotto, A. Gola, E. Chiesa, E. Lasalandra, F. Pasolini, M. Tronconi, T. Ungaretti, "A ±1-g dual-axis linear accelerometer in a standard 0.5-µm CMOS technology for high-sensitivity applications", IEEE Journal of Solid-State Circuits, 2003, Vol. 38, Issue 7, pp. 1292-1297.

[5] D. Yamane, T. Matsushima, T. Konishi, H. Toshiyoshi, K. Machida, K. Masu, "A dual-axis MEMS inertial sensor using multi-layered high-density metal for an arrayed CMOS-MEMS accelerometer", 2014 Symposium on Design, Test, Integration and Packaging of MEMS/MOEMS (DTIP), 2014, pp. 1-4.

[6] A. Garraud, A. Giani, P. Combette, B. Charlot, M. Richard, "A dual axis CMOS frontside bulk micromachined thermal accelerometer", 2010 Symposium on Design Test Integration and Packaging of MEMS/MOEMS (DTIP), 2010, pp. 67-72.

[7] W.N. Sharpe, B. Yuan, R. Vaidyanathan, R.L. Edwards, "Measurements of Young's modulus, Poisson's ratio, and tensile strength of polysilicon", Proceedings of IEEE Tenth Annual International Workshop on Micro Electro Mechanical Systems (MEMS'97), 1997, pp. 424-429.

[8] H. Kapels, R. Aigner, and J. Binder, "Fracture strength and fatigue of polysilicon determined by a novel thermal actuator", IEEE Transactions on Electron Devices, Vol. 47, No. 7, July 2000, pp. 1522-1528.